M&M: Unsupervised Mamba-based Mastoidectomy for Cochlear Implant Surgery with Noisy Data

Yike Zhang^a, Eduardo Davalos^a, Ange Lou^b, and Jack H. Noble^{a,b}

^aDept. of Computer Science, Vanderbilt University ^bDept. of Electrical and Computer Engineering, Vanderbilt University

ABSTRACT

Cochlear Implant (CI) procedures involve inserting an array of electrodes into the cochlea located inside the inner ear. Mastoidectomy is a surgical procedure that uses a high-speed drill to remove part of the mastoid region of the temporal bone, providing safe access to the cochlea through the middle and inner ear. In this paper, we propose a mamba-based method to synthesize the mastoidectomy volume using only the preoperative Computerized Tomography (CT) scan, where the mastoid is intact. We introduce an unsupervised learning framework designed to synthesize mastoidectomy. For model training purposes, this method uses postoperative CT scans to avoid manual data cleaning or labeling, even when the region removed during mastoidectomy is visible but affected by metal artifacts, low signal-to-noise ratio, or electrode wiring. Our approach estimates mastoidectomy regions with a mean Dice score of 0.70.

Keywords: Unsupervised Learning, Mamba-based, Noisy Data, Mastoidectomy, Cochlear Implant, CT

1. INTRODUCTION

Cochlear Implant (CI) procedures aim to restore hearing for patients with moderate-to-profound hearing disabilities.¹ These surgeries require performing a mastoidectomy, a procedure that involves removing part of the temporal bone to access the cochlea. Dillon et al.² proposed an automatic method using a bone-attached robot to perform the mastoidectomy. A validation study was designed to show the robot can accurately perform the procedures, preserving critical anatomical structures. However, in their proposed pipeline, the surgeon must manually identify the mastoidectomy-removed region on a preoperative Computerized Tomography (CT) scan, which can be time-consuming and laborious. In this work, we aim to develop an automatic mastoidectomy prediction method. Such a method could be useful for planning robotic surgery or for generating pre-operative visualizations of the surgical field for surgical training or pre-operative planning. We propose a deep learning-based segmentation network with an unsupervised training strategy.

Using CT scans acquired after CI, the shape of the actual mastoidectomy can be visualized in a postoperative CT. Postoperative CT scans are often acquired with low-dose cone beam scanners, which sometimes have lower resolution and increased artifacts, making them more difficult to inspect visually. These scans suffer from metal artifacts (bright white noise caused by implant components) and intensity heterogeneity due to fluid accumulation in the ear canal, posing challenges for deep learning models without hand-drawn labels. Traditional approaches for predicting the mastoidectomy-removed region using preoperative/postoperative CT pairs for training, such as Generative Adversarial Networks (GANs)³ and diffusion-based models,⁴ might not be suitable for our research goal due to the potential of generating undesired objects, such as fake electrodes and wires. Additionally, preoperative CTs have superior resolution compared to postoperative CTs in our dataset, delivering more detailed information for surgical planning and analysis. Therefore, a primary objective of our research is to design an effective framework to predict the mastoidectomy-removed region while preserving other original features of the preoperative CT and minimizing unnecessary alterations.

2. METHOD

In this work, we used a dataset of 751 preoperative and postoperative CT pairs from patients who underwent cochlear implantation. We randomly assigned 630 cases for training and validation, while reserving the rest for testing. We manually annotated the mastoidectomy-removed region in 32 randomly selected samples from the test dataset for evaluation. As preprocessing before training our method, the preoperative CT ρ and postoperative CT ω were aligned via rigid registration, and their intensity values were normalized. As shown in Fig. 1, the removed mastoid volume in ω tends to have lower intensities compared to surrounding tissue since it only contains air and soft tissue. Thus, we develop a model to predict the mastoidectomy region (represented as an inverted probability map δ) on ρ and make the predicted post-mastoid CT ($\rho \otimes \delta$) have higher similarity when compared with ω . The neural network shown in Fig. 2 is modeled as a function $f_{\theta}(\rho) = \delta$ using the state-of-the-art SegMamba-based⁵ neural network with a pretrained SAM-Med3D⁶ encoder as our feature extractor, where θ is the set of neural network parameters. In our model, we reduce the original CT dimensions to [160, 160, 64] by cropping around the ear regions using an ear anatomy segmentation neural network proposed in Zhang et al.⁷

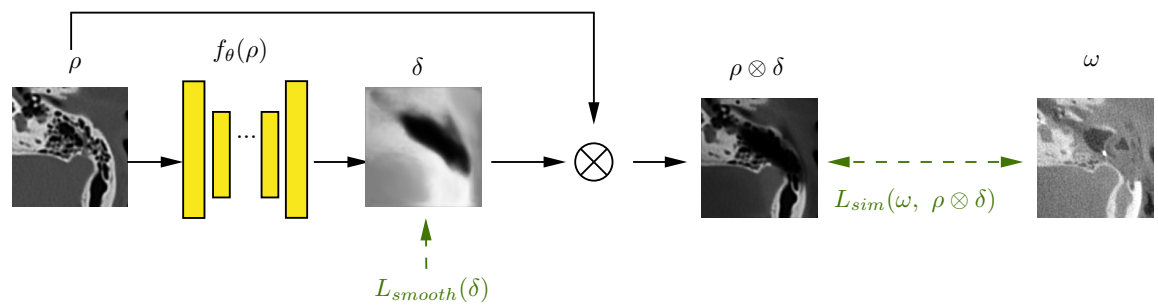


Figure 1: Framework overview. We compare the predicted mastoidectomy-removed region applied to the preoperative CT $\rho \otimes \delta$ against the postoperative CT ω using similarity-based loss function L_{msssim_cscc} . A smoothing term L_{smooth} is also applied to δ to further reduce noise output by network f_{θ} .

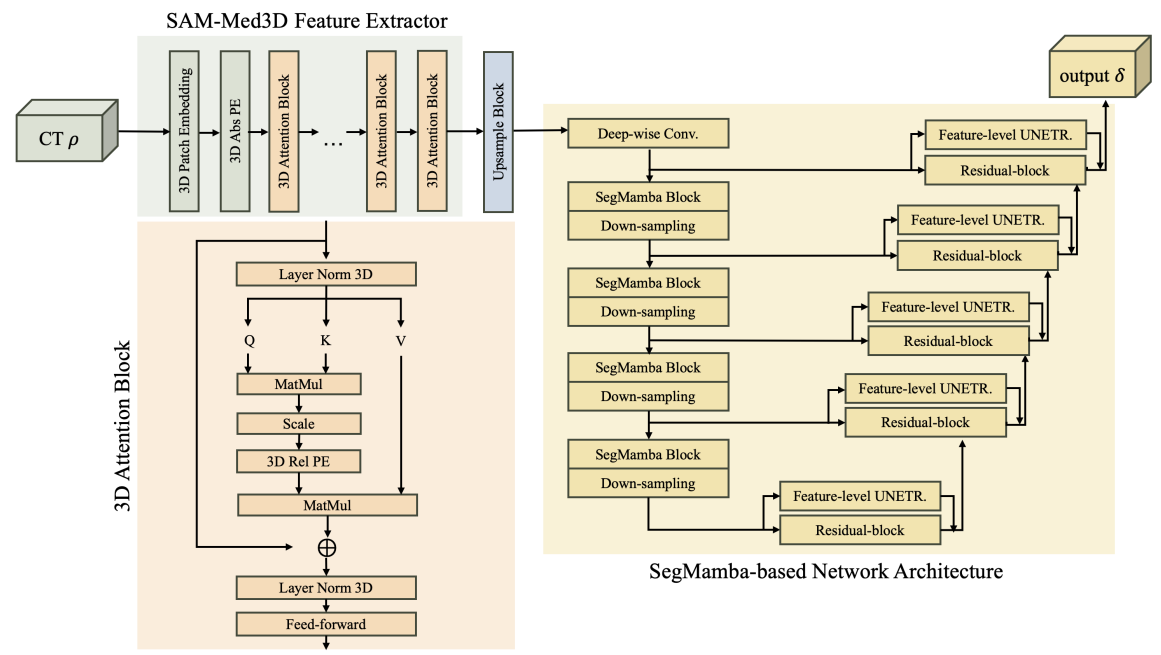


Figure 2: SegMamba-based Neural Network with pretrained SAM-Med3D Image Encoder

The Multi-Scale Structural Similarity Index (MS-SSIM)⁸ represents an improvement over the traditional

Structural Similarity Index (SSIM). This enhancement enables MS-SSIM to comprehensively evaluate the similarities and differences between two images across multiple scales. It effectively accommodates the wide variety of heterogeneity that can occur between two different images. We extend this metric with Squared Cross-Correlation (SCC)¹⁰ to quantify the overall structural similarity and distribution consistency between two image volumes $\rho \otimes \delta$ and ω . We propose two unsupervised loss functions L_{msssim_cscc} and L_{smooth} to train our model f_{θ} . L_{msssim_cscc} effectively minimizes the impact of undesired noise present in postoperative CTs. However, this loss function may result in fragmentation within the output probability map, thus we add the second loss function L_{smooth} to address the potential edge sharpness and encourage smoother value transitions in the output volume. The L_{smooth} is defined as $L_{smooth}(\delta) = \sum_{i=1}^{N} \|\nabla(\delta_i)\|^2$. We define $\frac{\partial \delta}{\partial x} \approx \delta(i_x + 1, i_y, i_z) - \delta(i_x, i_y, i_z)$, and the same rule applies to the $\frac{\partial \delta}{\partial y}$ and $\frac{\partial \delta}{\partial z}$. L_{msssim_cscc} performs across various scales, employing a multi-step down-sampling technique. Applying L_{msssim_cscc} alone effectively captures the target mastoidectomy region even when ω is contaminated by various noises.

$$L_{\text{msssim_cscc}}(\rho \otimes \delta, \omega) = 1 - [l_M(\rho \otimes \delta, \omega)]^{\alpha_M} \cdot \prod_{j=1}^{M} [c_j(\rho \otimes \delta, \omega) + SCC_j(\rho \otimes \delta, \omega)]^{\beta_j} [s_j(\rho \otimes \delta, \omega)]^{\gamma_j} \quad (1)$$

In Eq. 1, M represents the total number of scales at which the comparison is performed, and we assign M=5 in the loss function.⁸ α_M is the weight given to the luminance component at the coarsest scale. β_j refers to the weights assigned to the contrast components at each scale j. γ_j are the weights for the structure components at each scale j. $l(\rho \otimes \delta, \omega)$ is the luminance comparison function that measures the similarity in brightness between two image volumes. $c(\rho \otimes \delta, \omega)$ is the contrast comparison function that evaluates the similarity in structure or pattern between two image volumes. $s(\rho \otimes \delta, \omega)$ is the structure comparison function that represents the similarity in structure or pattern between two image volumes. SCC is being added to the contrast comparison function in this equation to enhance MS-SSIM capability to further maximize the distribution similarity at each scaling level. SCC is defined as:

$$SCC(\rho \otimes \delta, \omega) = \frac{\left(\sum_{i=1}^{N} \left[\left((\rho \otimes \delta)_{i} - \overline{\rho \otimes \delta} \right) (\omega_{i} - \overline{\omega}) \right] \right)^{2}}{\sum_{i=1}^{N} \left((\rho \otimes \delta)_{i} - \overline{\rho \otimes \delta} \right)^{2} \sum_{i=1}^{N} (\omega_{i} - \overline{\omega})^{2}},$$
(2)

where N is noted as the total number of pixels.

3. RESULTS

Fig. 3 shows the performance on eight test samples, with each column representing a test case. Our method predicts the mastoidectomy-removed region well in the majority of the cases, despite the challenge of manual annotation (about 1 hour per sample) due to the heterogeneity between preoperative and postoperative CTs and the variability in mastoidectomy-removed regions' shapes and sizes. The last column shows the case with the worst Dice score using our proposed method. In this case, the mastoid region in that preoperative CT scan is unusually sparse compared to the other samples in our test dataset. This leads to a predicted mastoidectomy region that is smaller than the ground truth using the unsupervised method. Table 1 compares key metrics of widely-used transformer-based networks and U-Net-based networks, including SwinUNetr, 11 UNETR, 12 the U-Net+ 13 / U-Net14 network using ImageNet15 pretrained weights, and our proposed mamba-based method. Fig. 4 shows our method's ablation study with different loss functions. L_{msssim_cscc} is our proposed loss term, while L_{msssim_scc} refers to adding Eq. 2 to the s($\rho \otimes \delta$, ω) structural similarity function instead of the c($\rho \otimes \delta$, ω) contrast comparison function in MS-SSIM (Eq. 1). L_{msssim} indicates the original MS-SSIM loss function.

4. BREAKTHROUGH WORK (THIS WORK HAS NOT BEEN PRESENTED ELSEWHERE)

Our paper introduces a novel unsupervised mamba-based deep learning framework and a new loss function for mastoidectomy in CI surgery using highly noisy original postoperative CT datasets. We propose an innovative approach to train neural networks with only noisy data, eliminating the need for extensive manual cleaning and labeling. This methodology can potentially extend to other surgical procedures where manual annotations are challenging and time-consuming.

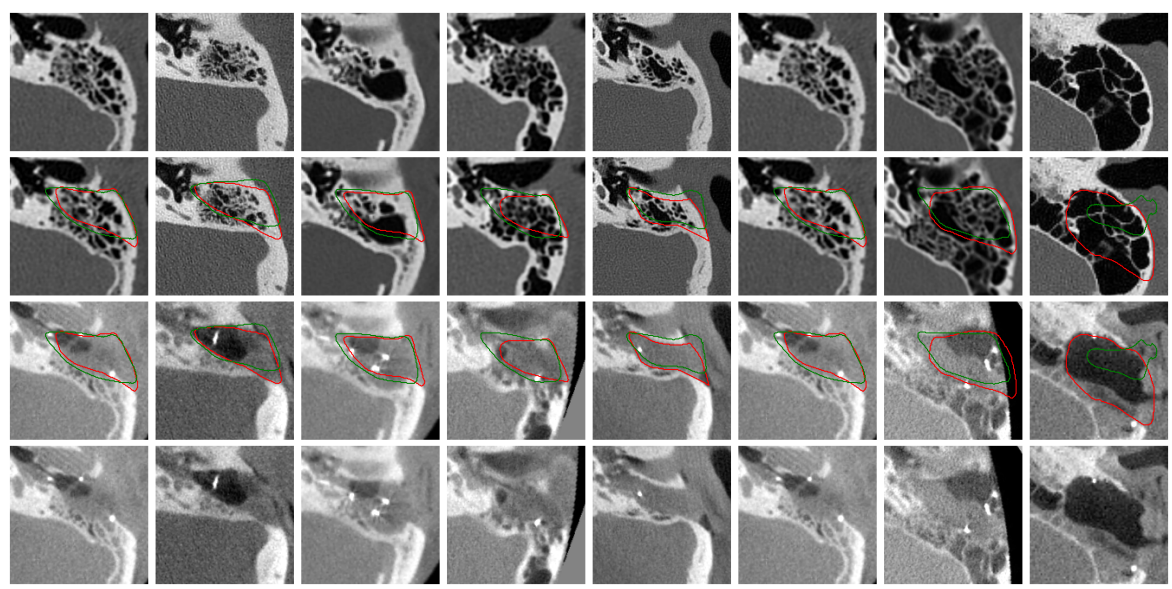


Figure 3: Qualitative Performance Evaluation. The first row displays preoperative CT scans. The second row overlays predicted mastoidectomy-removed areas (green) and ground truth (red) on preoperative CTs. The third row shows these contours on postoperative CT scans, and the final row displays the postoperative CTs.

Methods	Dice ↑	IoU ↑	Acc ↑	Pre ↑	Sen ↑	Spe ↑	HD95% ↓	ASD ↓
UNet ¹⁴	0.5432	0.3867	0.9203	0.8215	0.4319	0.9877	26.1439	5.0094
UNet++ ¹³	0.6527	0.4931	0.9230	0.7937	0.6010	0.9671	20.3570	6.2326
UNetr ¹²	0.5608	0.4020	0.9263	0.8734	0.4246	0.9936	20.1116	6.5478
SwinUNetr ¹¹	0.6426	0.4834	0.9317	0.8506	0.5293	0.9885	17.2194	5.6297
Our Method	0.7019	0.5450	0.9375	0.7970	0.6444	0.9795	17.3515	4.1585

Table 1: Performance comparison between Transformer/U-Net-based network and Mamba-based network

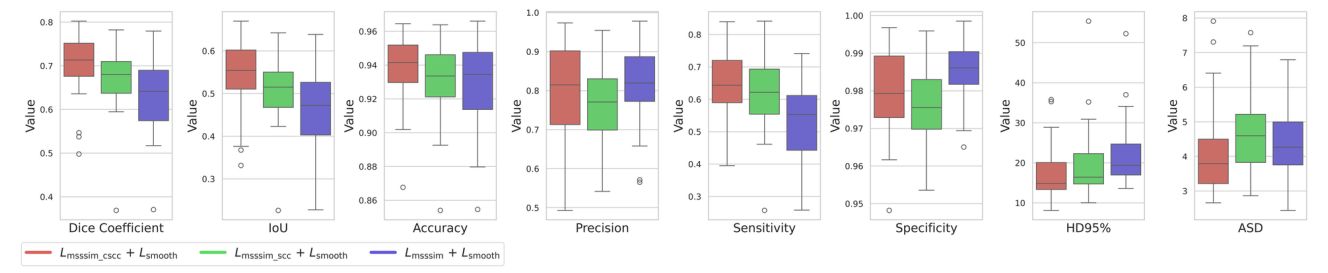


Figure 4: Ablation Study: comparing performance across different loss functions.

5. DISCUSSION AND CONCLUSION

The proposed unsupervised learning framework predicted the mastoidectomy-removed region with a mean Dice coefficient of 0.70. These results show promise that our self-supervised network can assist surgeons in planning a mastoidectomy without requiring extensive and laborious manual annotation.

REFERENCES

- [1] Labadie, R. and Noble, J., "Preliminary results with image-guided cochlear implant insertion techniques," *Otol Neurotol* **39**, 922–928 (Aug 2018).
- [2] Dillon, N. P., Balachandran, R., Fitzpatrick, J., Siebold, M., Labadie, R., Wanna, G., Withrow, T., and Webster, R., "A compact, bone-attached robot for mastoidectomy.," *Journal of medical devices* **9 3**, 0310031–310037 (2015).

- [3] You, C., Li, G., Zhang, Y., Zhang, X., Shan, H., Li, M., Ju, S., Zhao, Z., Zhang, Z., Cong, W., et al., "Ct super-resolution gan constrained by the identical, residual, and cycle learning ensemble (gan-circle)," *IEEE transactions on medical imaging* **39**(1), 188–203 (2019).
- [4] Dhariwal, P. and Nichol, A., "Diffusion models beat gans on image synthesis," CoRR abs/2105.05233 (2021).
- [5] Xing, Z., Ye, T., Yang, Y., Liu, G., and Zhu, L., "Segmamba: Long-range sequential modeling mamba for 3d medical image segmentation," (2024).
- [6] Wang, H., Guo, S., Ye, J., Deng, Z., Cheng, J., Li, T., Chen, J., Su, Y., Huang, Z., Shen, Y., Fu, B., Zhang, S., He, J., and Qiao, Y., "Sam-med3d," (2023).
- [7] Zhang, Y. and Noble, J. H., "Self-supervised registration and segmentation on ossicles with a single ground truth label," in [Medical Imaging 2023: Image-Guided Procedures, Robotic Interventions, and Modeling], Linte, C. A. and Siewerdsen, J. H., eds., 12466, 124660X, International Society for Optics and Photonics, SPIE (2023).
- [8] Wang, Z., Simoncelli, E., and Bovik, A., "Multiscale structural similarity for image quality assessment," in [The Thrity-Seventh Asilomar Conference on Signals, Systems & Computers, 2003], Conference Record of the Asilomar Conference on Signals, Systems and Computers 2, 1398 1402 Vol.2 (12 2003).
- [9] Wang, Z., Bovik, A., Sheikh, H., and Simoncelli, E., "Image quality assessment: from error visibility to structural similarity," *IEEE Transactions on Image Processing* **13**(4), 600–612 (2004).
- [10] Avants, B. B., Epstein, C. L., Grossman, M., and Gee, J. C., "Symmetric diffeomorphic image registration with cross-correlation: evaluating automated labeling of elderly and neurodegenerative brain," *Medical Image Analysis* 12(1), 26–41 (2008).
- [11] Hatamizadeh, A., Nath, V., Tang, Y., Yang, D., Roth, H., and Xu, D., "Swin unetr: Swin transformers for semantic segmentation of brain tumors in mri images," (2022).
- [12] Hatamizadeh, A., Tang, Y., Nath, V., Yang, D., Myronenko, A., Landman, B., Roth, H., and Xu, D., "Unetr: Transformers for 3d medical image segmentation," (2021).
- [13] Zhou, Z., Siddiquee, M. M. R., Tajbakhsh, N., and Liang, J., "Unet++: Redesigning skip connections to exploit multiscale features in image segmentation," *IEEE Transactions on Medical Imaging* (2019).
- [14] Ronneberger, O., Fischer, P., and Brox, T., "U-net: Convolutional networks for biomedical image segmentation," *CoRR* abs/1505.04597 (2015).
- [15] Deng, J., Dong, W., Socher, R., Li, L.-J., Li, K., and Fei-Fei, L., "Imagenet: A large-scale hierarchical image database," in [2009 IEEE Conference on Computer Vision and Pattern Recognition], 248–255 (2009).